REGULAR ARTICLE

blood advances

Next-generation sequencing of idiopathic multicentric and unicentric Castleman disease and follicular dendritic cell sarcomas

Alexandra Nagy,[1] Aparna Bhaduri,[2] Nahid Shahmarvand,[1] Jahanbanoo Shahryari,[1] James L. Zehnder,[1] Roger A. Warnke,[1] Tariq Mughal,[3,4] Siraj Ali,[3] and Robert S. Ohgami[1]

[1]Department of Pathology, Stanford University, Stanford, CA; [2]Department of Regeneration Medicine, University of California San Francisco, San Francisco, CA; [3]Foundation Medicine Inc, Cambridge, MA; and [4]Department of Medicine, Tufts University Medical Center, Boston, MA

Key Points

- A single rare DNMT3A mutation and recurrent amplification of ETS1, PTPN6, and TGFBR2 are identified in iMCD and UCD.
- Genetic alterations in oncogenes, tumor suppressors, and chromatin-remodeling genes are seen in FDCS.

Castleman disease (CD) is a rare lymphoproliferative disorder subclassified as unicentric CD (UCD) or multicentric CD (MCD) based on clinical features and the distribution of enlarged lymph nodes with characteristic histopathology. MCD can be further subtyped based on human herpes virus 8 (HHV8) infection into HHV8-associated MCD, HHV8$^-$/idiopathic MCD (iMCD), and polyneuropathy, organomegaly, endocrinopathy, monoclonal gammopathy, and skin change (POEMS)–associated MCD. In a subset of cases of UCD, an associated follicular dendritic cell sarcoma (FDCS) may be seen. Although numerous reports of the clinical and histologic features of UCD, MCD, and FDCS exist, an understanding of the genetic and epigenetic landscape of these rare diseases is lacking. Given this paucity of knowledge, we analyzed 15 cases of UCD and 3 cases of iMCD by targeted next-generation sequencing (NGS; 405 genes) and 3 cases of FDCS associated with UCD hyaline vascular variant (UCD-HVV) by whole-exome sequencing. Common amplifications of *ETS1*, *PTPN6*, and *TGFBR2* were seen in 1 iMCD and 1 UCD case; the iMCD case also had a somatic *DNMT3A* L295Q mutation. This iMCD patient also showed clinicopathologic features consistent with a specific subtype known as Castleman-Kojima disease (thrombocytopenia, anasarca, fever, reticulin fibrosis, and organomegaly [TAFRO] clinical subtype). Additionally, 1 case of UCD-HVV showed amplification of the cluster of histone genes on chromosome 6p. FDCS associated with UCD-HVV showed mutations and copy number changes in known oncogenes, tumor suppressors, and chromatin structural-remodeling proteins.

Introduction

Castleman disease (CD), also known as angiofollicular lymphoid hyperplasia, giant lymph node hyperplasia, and lymphoid hamartoma, is a rare lymphoproliferative disorder.[1] Based on clinical features and the distribution of enlarged lymph nodes with characteristic histopathology, CD can be subclassified into localized unicentric CD (UCD) or multicentric CD (MCD). MCD is further subtyped based on human herpes virus 8 (HHV8) status to either HHV8-associated MCD or HHV8$^-$ MCD. HHV8$^-$ MCD is further subdivided into idiopathic MCD (iMCD) or polyneuropathy, organomegaly, endocrinopathy, monoclonal gammopathy, and skin change (POEMS)–associated MCD. HHV8-associated MCD occurs due to uncontrolled HHV8 infection in individuals with HIV infection or other causes of immunodeficiency. Histologically, UCD can be subdivided into a hyaline vascular variant (UCD-HVV) and a plasma cell variant (UCD-PCV), as well as a mixed variant (UCD-MV), which shares morphologic features of both UCD-HVV and UCD-PCV. The pathogenesis of iMCD and UCD is still not well understood.[2] In 2010,

Submitted 6 July 2017; accepted 30 January 2018. DOI 10.1182/bloodadvances.2017009654.

The full-text version of this article contains a data supplement.

Takai et al[3] described 3 patients with findings consistent with iMCD and a further characteristic constellation of clinical features including thrombocytopenia, anasarca, fever, reticulin fibrosis, and organomegaly (TAFRO): a clinical subtype of iMCD also known as Castleman-Kojima syndrome.[4,5] Since then, numerous patients have been identified; some reportedly respond well to immunosuppressive therapy, specifically cyclosporine and prednisolone.

In recent years, cytogenetic and molecular studies have demonstrated clonal abnormalities in UCD and iMCD.[6,7] Recently, studies of a rare clinically aggressive mesenchymal tumor, follicular dendritic cell sarcoma (FDCS), have been performed with next-generation sequencing (NGS) and identified somatic mutations in a subset of cases.[8,9] However, the mutational landscape of MCD and UCD, and FDCS associated with UCD-HVV remains an enigma. As such, we performed targeted sequencing of lymph node tissue specimens from patients with iMCD and UCD as well as whole-exome sequencing (WES) of FDCS to delineate the underlying molecular aberrations that may have a pathogenetic role.

Materials and methods

Patient cohort

Fifteen cases of UCD, 3 cases of iMCD (2 of 3 cases showed clinicopathologic features further consistent with the TAFRO clinical subtype of iMCD), and 3 cases of FDCS associated with UCD-HVV, diagnosed between 2002 and 2015, were identified from the archives of the Department of Pathology, Stanford University Medical Center (Stanford, CA). All cases and slides were reviewed and diagnoses confirmed. Patient medical record charts were reviewed, and clinical and laboratory data as well as treatment data were reviewed by Stanford specialists in hematology and hematopathology (R.S.O., J.L.Z., T.M., and R.A.W.). This study was approved by Stanford University's Institutional Review Board.

High-throughput sequencing and analysis

NGS with alignment, single-nucleotide variant, copy-number variant (CNV), translocation, and indel analysis of DNA data were performed as previously described; translocations were evaluated using the Fusion and Chromosomal Translocation Enumeration and Recovery Algorithm (FACTERA).[10-12] DNA was isolated from lymph node tissues using the QIAamp DNA FFPE tissue kit (Qiagen). Targeted exome sequencing of 405 genes (FoundationOne [F1]) was performed for the 15 UCD and 3 iMCD cases and WES for the 3 FDCSs associated with UCD-HVV cases. Targeted hybrid-capture NGS (F1; Foundation Medicine Inc) of 405 genes was performed as previously described.[12] In brief, 50 to 200 ng of DNA was fragmented before library construction by sonication and adaptor ligated libraries created. Sanger sequencing of select genes was performed at an early stage to evaluate DNA quality and also assure that NGS assays were performing as anticipated. Solution hybridization was performed using pools of biotinylated DNA baits. Libraries were pooled and sequenced on an Illumina HiSeq2500. A median exon coverage of 150 to 250 was considered qualified. A mutant allele frequency (MAF) cutoff of 1% for known somatic variants (based on COSMIC v62) and 5% for novel somatic variants was followed; for indels, the MAF cutoff was 3% for known somatic variants and 10% for novel somatic variants. One hundred base-pair paired-end WES on 3 FDCS cases was performed using the Sureselect whole-exome V5 kit (Agilent Technologies) at an average depth of coverage of 180-fold. Alignment was performed using Burrows-Wheeler Aligner –maximum exact matches (BWA-MEM) with further analysis performed using GATK (version 3), Varscan2, and SNNPET (Agilent Technologies). For all samples, callers were run with default settings in individual sample analysis modes. To call a mutation, 20× coverage of the base analyzed (as defined by the mutation caller itself) was required, as well as coverage in both the forward and reverse directions. Unequal representation of read counts (>80%/20% split) were additionally discounted. A minimum allele frequency of 0.05 was required in addition to the coverage restriction. Indel analysis was performed with GATK, SNNPET, and Varscan2. GATK was run according to the best practices guidelines and VarScan2 and SNNPET were run with default parameters. The variant filtration detailed in this section was similarly applied to indel analysis. Annotation of variants was performed using Surecall (version 3.5.1.46; Agilent Technologies) and Seattleseq (version 9.10; University of Washington, Seattle WA). Variants were additionally curated using Exome Aggregation Consortium (EXAC), Clinvar, 1000 genomes, and Exome Variant Server (EVS) and The Cancer Genome Atlas TCGA database. CNV analysis was performed with Surecall and CNVSeq, both run with default parameters, and analysis was performed on the "hits" file. WES data from 5 reactive lymph nodes and targeted sequencing data (405 genes) from an additional 73 reactive lymph nodes were additionally used as negative controls; pathogenic somatic mutations or gene amplifications at default threshold parameters were not seen.

Sanger sequencing

Sanger sequencing was performed on a subset of genes to confirm single-nucleotide variants identified in WES and targeted sequencing (supplemental Table 1) with concordance of 100%.

Statistical and hierarchical gene relational analysis

Student *t* and Fisher exact tests were performed as previously described. Unsupervised hierarchical gene cluster analysis was performed using Morpheus (Broad Institute, Cambridge, MA).

Results

Patients

Twenty-one patients were included in this study: 15 cases of UCD, 3 cases of iMCD, and 3 cases of FDCS associated with UCD-HVV.[13] All cases were negative for HHV8 and HIV. Three cases of FDCSs arising in the setting of UCD were also studied; 2 male and 1 female, 27, 73, and 55 years of age. The clinical characteristics of the cases are shown in Tables 1 and 2.

Mutational analysis

We performed F1 NGS of 405 genes on 15 UCD and 3 iMCD cases to an average depth of 800-fold coverage and observed a somatic mutation in 1 patient with iMCD-PC (case 3), who also met criteria for the TAFRO clinical subtype, in DNMT3a (L295Q) at a variant allele frequency (VAF) of 9%, which was reverified by repeating targeted sequencing (Table 3; Figure 1). This mutation was not seen in paired normal control bone marrow tissue, peripheral blood, nor in uninvolved adipose tissue directly adjacent to the lymph node by Sanger sequencing or targeted NGS. The mutation was not listed as a germ line variant in any servers (EXAC,

Table 1. UCD and MCD case demographics

Case	Subtype	Sex	Age, y	Site of involvement/ lymphadenopathy	Clinical sequelae	Organomegaly	Viral status	Laboratory results	Treatment	Status (time of follow-up)
1	UCD-HVV	M	26	Interaortocaval right lower quadrant	Isolated adenopathy	None	HIV$^-$, HHV8$^-$	NS	Resection	Alive (10 y)
2	UCD-HVV	M	35	Head/right neck	Isolated adenopathy	None	HHV8$^-$	NS	Resection	Alive (2 y)
3	iMCD-PC (2 major criteria; 8 minor criteria)	F	70	Axillary, inguinal, mediastinal, intraabdominal lymphadenopathy	Fatigue, edema and pleural effusions; TAFRO syndrome	None	HHV8$^-$, HIV$^-$, EBV$^-$	ESR, 98 mm/h; CRP, 11.16 mg/L; Hgb, 8.1 g/dL; PLT, 49 × 10^9/L; IgG 2230 mg/dL; albumin, 2.6 g/dL; eGFR 36 mL/min/m^2	Resection, Rituximab-Etoposide/Siltuximab	Alive (2 y)
4	UCD-HVV	F	40	Left axillary and subpectoral lymphadenopathy	Localized adenopathy	None	HHV8$^-$, HIV$^-$, EBV$^-$	CRP, 3.1 mg/dL; Hgb, 9.4 g/dL	Resection	Alive (4 y)
5	UCD-MV	F	59	Bilateral cervical lymphadenopathy/ nasopharyngeal mass	Extensive multinodal adenopathy	None	HHV8$^-$, HIV$^-$, EBV$^-$		Resection, tocilizumab	Alive (4 y)
6	UCD-PCV	F	57	Left neck lymphadenopathy	Extensive localized adenopathy	None	HHV8$^-$, EBV$^-$	CRP, 2.7 mg/dL	Resection, rituximab	Alive (5 y)
7	UCD-HVV	F	28	Left neck lymphadenopathy	Localized adenopathy	None	HIV$^-$, HHV8$^-$	NS	Resection	Alive (5 y)
8	iMCD-PC (2 major criteria; 4 minor criteria)	M	35	Large anterior mediastinal mass, cervical lymphadenopathy	Weight loss, night sweats, fatigue	None	HHV8$^-$, HIV$^-$, EBV$^-$	Hgb, 12.1 g/dL; PLT, 568 × 10^9/L; Hypergamma-globulinemia	Resection	Alive (3 y)
9	UCD-HVV	M	30	Retroperitoneal lymphadenopathy	Isolated adenopathy	None	HHV8$^-$	NS	Resection	Alive (6 y)
10	UCD-HVV	F	42	Left pelvic lymphadenopathy	Isolated adenopathy	None	HHV8$^-$, HIV$^-$	NS	Resection, XRT	Alive (4 y)
11	iMCD-M (2 major; 7 minor criteria)	M	21	Diffuse retroperitoneal, inguinal lymphadenopathy	TAFRO syndrome; fatigue, fever, weight loss; hepatomegaly; edema	Hepatospleno-megaly	HHV8$^-$, EBV$^-$, HIV$^-$	CRP, 16.4 mg/dL; Hgb, 7.9 g/dL; PLT, 77 K/μL; eGFR, 43 mL/min/m^2	Siltuximab, rituximab	Alive (2 y)
12	UCD-HVV	F	17	Neck lymphadenopathy	Localized adenopathy	N/A	HHV8$^-$	NS	Resection, localized XRT	Alive (11 y)
13	UCD-HVV	M	30	Anterior mediastinal mass	Localized mass	N/A	HHV8$^-$	NS	Resection, steroids	Alive (4 y)
14	UCD-HVV	M	36	Neck lymphadenopathy	Localized mass	None	HHV8$^-$	NS	Resection, XRT	Alive (1 y)
15	UCD-HVV	F	17	Left adnexal mass	Localized mass	None	HHV8$^-$	NS	Resection	Alive (4 y)
16	UCD-HVV	F	24	Anterior mediastinal mass	Fatigue; localized mass	N/A	HHV8$^-$	NS	Resection	Alive (13 y)
17	UCD-HVV	F	14	Paratracheal mediastinal mass	Localized mass	N/A	HHV8$^-$	NS	Resection	Alive (8 y)
18	UCD-HVV	F	29	Pelvic mass	Isolated adenopathy	None	HHV8$^-$	NS	Resection	Alive (2 y)

CRP, C-reactive protein; EBV, Epstein-Barr virus; eGFR, estimated glomerular filtration rate; ESR, erythrocyte sedimentation rate; F, female; Hgb, hemoglobin; IgG, immunoglobulin G; iMCD-M, HHV8$^-$/iMCD with mixed pathology; iMCD-PC, HHV8$^-$/iMCD with plasmacytic pathology; M, male; N/A, not available; NS, not significant; PLT, platelet; XRT, radiotherapy.

Table 2. FDCS case demographics

Case	Sex	Age, y	Site of involvement	Viral status	Treatment/Clinical course	Status
19	M	27	Right inguinal lymphadenopathy	HHV8$^-$	Excision	Alive (3 y)
20	F	73	Left neck mass	HHV8$^-$; EBV$^-$	N/A	N/A
21	M	55	Epigastric lymph nodes and liver masses	HHV8$^-$	Excision and CHOP	Alive (2 y)

CHOP, cyclophosphamide, doxorubicin, vincristine, prednisone.

Clinvar, 1000 genomes, and EVS). Our analyses did not reveal somatic mutations in the remaining 17 of 18 UCD and iMCD cases. We additionally performed WES to an average depth of 180-fold coverage on 3 FDCSs associated with UCD-HVV. These 3 cases showed 3 to 5 somatic mutations per case in known oncogenes, tumor suppressors, and chromatin-remodeling proteins (Table 3; Figure 1). Notable mutations included those in known oncogenes and tumor suppressors such as *SETD2* (A1896E) and *WDR55/DND1* (E334K), and chromatin modifiers such as *NCAPH* (E287K) and *TOP3B* (E623K). Mutations in genes frequently mutated in subsets of hematopoietic neoplasms, such as *ZBTB7a* (K424N), also mutated in acute myeloid leukemia,[14] and *STAT3* (D170N), a gene frequently mutated in T-cell large granular lymphocytic leukemia and chronic natural killer (NK) lymphoproliferative disorders, was also present in 1 FDCS case (Table 3).[15-17] No somatic mutations were recurrently seen among UCD and iMCD cases or with FDCS cases.

We identified CNV changes that met our threshold parameters in 3 of our UCD and iMCD cases; their histology is also shown in Figure 2. Case 14 (UCD-HVV) had copy-number gains in the *HIST1H* genes. Interestingly, 2 cases, case 3 (HHV8$^-$/iMCD with plasma cell histology [iMCD-PC]), and case 5 (UCD-MV), showed common copy-number gains in the genes *PTPN6*, *ETS1*, and *TGFBR2* (Figure 1). We also identified multiple CNV changes in our FDCS cases (Table 4). Of our FDCS cases, case 19 displayed mainly losses, whereas case 20 showed both copy-number gains and losses; case 21 presented with mainly copy-number gains. Overlapping CNVs were seen between case 19 and case 20, which both showed losses in *BRAF*; additionally, *FANCB* was altered in both case 19 and case 20 though 1 was loss (case 19) and the other gain (case 20). CNVs in genes previously described as altered in FDCS, such as *NFKBI* and *JAK2*, were additionally present.[9] Finally, loss of several *HISTH* genes was seen in case 20. Translocations were not identified in cases by NGS.

Discussion

Our study of UCD and iMCD, and FDCS associated with UCD-HVV identified a *DNMT3a* L295Q mutation in a single case of iMCD-PC, which additionally met criteria for the TAFRO clinical subtype of iMCD, and recurrent copy-number alterations in 1 case of iMCD and 1 case of UCD, as well as numerous nonrecurrent mutations and copy-number alterations in FDCS associated with UCD-HVV. Although the majority of cases of UCD and iMCD did not show somatic mutations in the 405 genes sequenced, one 70-year-old patient with iMCD-PC (case 3), and the TAFRO clinical subtype, showed a mutation in *DNMT3A*, a DNA methyltransferase commonly mutated in myeloid neoplasms as well as nonhematopoietic neoplasms.[18,19] This mutation was not seen in matched normal control tissue (bone marrow, peripheral blood, or adjacent uninvolved adipose tissue), suggesting it is an acquired mutation. This specific *DNMT3A* L295Q mutation has also been described in a case of acute myeloid leukemia (AML) and the mutation is located in the Proline-Tryptophan-Tryptophan-Proline (PWWP) domain, a critical region for DNA binding.[20] Mutations in the PWWP domain have been described to result in defects in the ability of DNMT3A to methylate DNA due to loss of chromatin targeting by DNMT3A.[21-24] In vivo studies in mice, assessing the loss of DNMT3A function, have shown global defects in hypomethylation and its critical role in impairing hematopoietic stem cell differentiation although resulting in expansion of hematopoietic stem cell numbers.[23] Data support *DNMT3A* functioning as a tumor suppressor in many cancer systems[19] and such may be true here; however, further in vivo studies are necessary to understand how this specific mutation may affect the survival and/or proliferation of affected cells, and cytokine production observed in iMCD.[18,19] Based on our understanding of iMCD and the function of DNMT3A as discussed in this paragraph, one possible hypothesis is that the L295Q DNMT3A mutation is present in an undefined population of clonal cells, possibly a stromal cell population, and results in increased proliferation of this population of cells. We speculate that a paraneoplastic syndrome then ensues potentially from primary production of cytokines (interleukin-6 [IL-6], vascular endothelial growth factor) by this cellular population. Indeed, in a recent paper by Yang et al,[25] the authors demonstrate that DNMT3A overexpression in human fibroblasts results in suppression of IL-6 expression; that deletion of DNMT3A conversely might increase IL-6 expression was not addressed, but certainly the results from Yang et al are consistent with this possibility. Subsequently IL-6 can then perhaps drive the polyclonal plasmacytosis seen in iMCD.[26] Alternatively, clonal proliferation of this undefined population of cells may directly stimulate an autoimmune system response, and the overall sequelae of iMCD. Yet another possibility is that this DNMT3A mutation is a passenger mutation and not a true driver mutation (though present in the key neoplastic population), and the true driver mutation was not identified by our targeted sequencing approach. A final possibility is that this mutation is actually present in the polyclonal lymphoid population, though this is unlikely because adjacent uninvolved fat, where lymphoid and plasma cells were present as well as marrow and peripheral blood, did not show a *DNMT3A* mutation.[23]

We also considered that this specific *DNMT3A* L295Q mutation might be related to clonal hematopoiesis of indeterminant potential (CHIP), or one seen in idiopathic cytopenias of undetermined significance, but this mutation was not seen in patient-matched control bone marrow biopsy tissue or peripheral blood. Additionally, this patient did not demonstrate any pathologic evidence for a myeloid neoplasm in a concurrent bone marrow biopsy, and has not developed a myeloid neoplasm over a 2-year period of follow-up. Although *DNMT3A* mutations are overall one of the more frequent mutations in CHIP, the frequency of non-R882 somatic mutations in

Table 3. Somatic mutations identified in a case of HHV8$^-$/iMCD (case 3) and FDCSs arising from UCD

Case	Gene	Position	VAF, %	Nucleotide change	Type of mutation	AA change	CADD	Pathway
CD								
3	*DNMT3A*	Chr2:25470590	9	T>A	Missense	L295Q	Unknown	DNA methylation
FDCSs								
19	*IL17RD*	Chr3:57135385	38	T>C	Missense	I329T	22.2	FGFR pathway
19	*NUDT4*	Chr12:93772182	38	C>G	Missense	S28R	13.7	Intracellular trafficking
19	*CABIN1*	Chr22:24479275	39	A>G	Missense	Y898C	19.25	Chromatin structure, T-cell receptor mediated signaling
20	*ZBTB7A*	Chr19:4048233	14	C>G	Missense	K424N	17.6	Oncogene; regulation of glycolysis
20	*DRD5*	Chr4:9783892	40	T>A	Missense	I80N	19.7	Dopamine; Other
20	*TOP3B*	Chr22:22311800	40	C>T	Missense	E623K	16.2	Topoisomerase; DNA structure
21	*STAT3*	Chr17:40490791	26	C>T	Missense	D170N	25	Transcription
21	*WDR55/DND1*	Chr5:140050940	15	C>T	Missense	E334K	12.6	Oncogene; translational regulation
21	*NCAPH*	Chr2:97017707	20	A>G	Missense	E287K	13.2	Chromatin structure
21	*SETD2*	Chr3:47125583	24	G>T	Missense	A1896E	16.2	Tumor suppressor; histone methyltransferase
21	*MARCH7*	Chr2:160605297	20	A>G	Missense	N443S	16.3	Ubiquitin ligase

AA, amino acid; CADD, Combined Annotation Dependent Depletion; FGFR, fibroblast growth factor receptor.

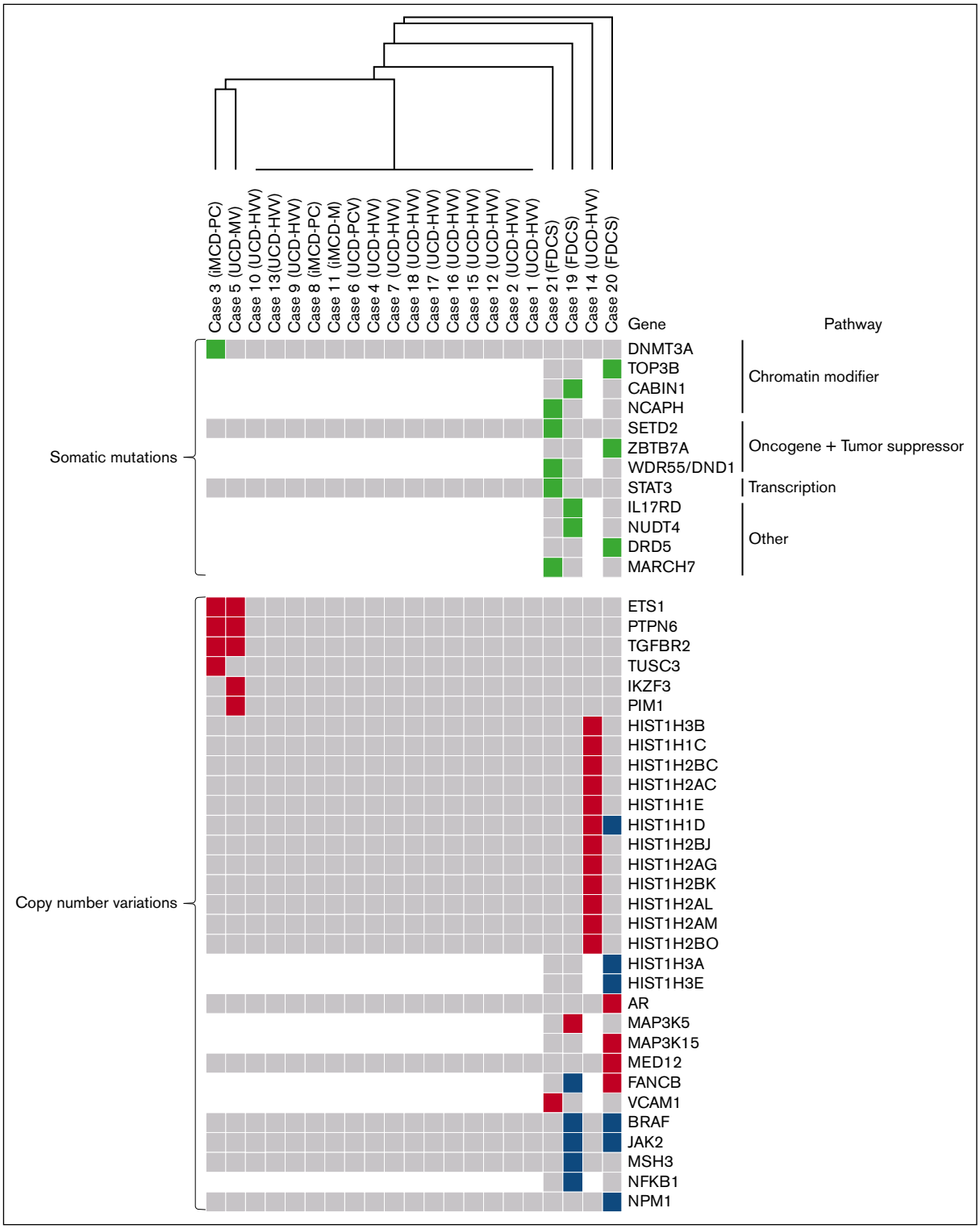

Figure 1. Somatic gene mutations and CNVs in cases of UCD and HHV8^{-}/iMCD and FDCS associated with UCD-HVV. Depicted is an unsupervised hierarchical cluster analysis of genetic alterations in UCD, iMCD, and FDCS associated with UCD-HVV. The top portion depicts somatic mutations in all UCD, iMCD, and FDCS cases (green boxes indicate genes mutated in individual cases); the bottom portion depicts CNVs in all UCD, iMCD, and FDCS cases. CNV gains are in red, whereas CNV losses are in blue. Gray boxes indicate genes without abnormalities. White areas/boxes indicate genes not evaluated by targeted sequencing. iMCD-M, HHV8^{-}/iMCD with mixed histology; iMCD-PC, HHV8^{-}/iMCD with plasma cell histology.

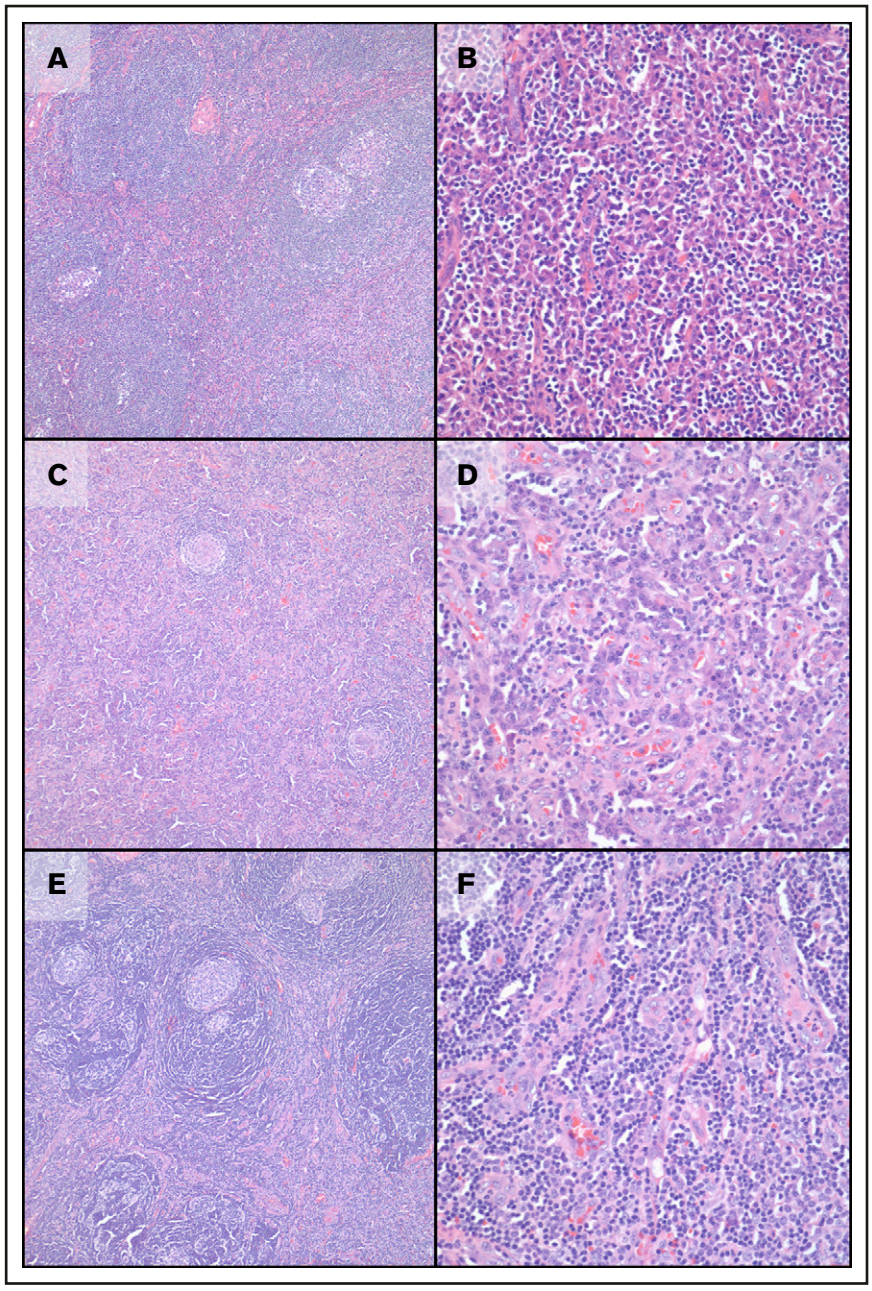

Figure 2. Morphologic features of cases of UCD and MCD with genetic abnormalities. (A-B) Case 3, HHV8$^-$/iMCD with plasmacytic histology. At low-power magnification, regressed follicles are seen with onion skinning of mantle zones and "twinning" of follicles; increased plasma cells are clearly seen in interfollicular regions with mild vascularity. (C-D) Case 5, UCD-MV. At low-power magnification, regressed follicles are seen with onion skinning of mantle zones along with increased vascularity in interfollicular regions. At high-power magnification, increased plasma cells are clearly seen along with increased vascularity. (E-F) Case 14, UCD-HVV. At low-power magnification, regressed follicles are seen with prominent onion skinning of mantle zones and "twinning" of follicles. At high-power magnification, increased vascularity is present without increased plasma cells. In all panels, images on cases are taken in sequence at ×100 (left) and ×400 (right) magnification; all images are from hematoxylin and eosin–stained slides.

patients without hematologic malignancies is <2% in 70-year-olds and this L295Q mutation has not been described in any CHIP studies evaluating *DNMT3A* in >30 000 individuals.[27,28] The only instance of this mutation identified to date, to our knowledge, has been in a case of AML as mentioned in the previous paragraph.[20] That a mutation in *DNMT3A* might underlie at least a subset of cases of iMCD is intriguing, though we did not identify it recurrently in the other iMCD or UCD cases.

To understand the possible association between UCD-HVV and FDCS, we analyzed the mutational landscape of FDCS associated with UCD-HVV by WES. Although no recurrent somatic mutations were seen between cases of FDCS, not surprisingly, mutations in oncogenes and genes known to be critical in tumorigenesis were identified: specifically, mutations in tumor suppressors such as *SETD2* (A1896E) and *WDR55/DND1* (E334K), and chromatin modifiers such as *NCAPH* (E287K) and *TOP3B* (E623K). Additionally, among our FDCS cases, mutations in *ZBTB7A* (K424N) and *STAT3* (D170N) were seen. A known oncogene, *ZBTB7A*, plays a key role in the development from lymphoid progenitors into B-cell lineage and is recurrently mutated in AML,[14,29] and *STAT3* is a transcription factor mutated in NK, T-cell, and B-cell disorders.[30-32] We also evaluated for previously published mutations seen in FDCS not associated with UCD-HVV, but recurrent mutations were not seen between those prior studies and ours.[9] In some sense, this is not entirely surprising as the histology and specific immunophenotypic expression patterns of FDCS can be somewhat diverse.[33] One gene mutation of major interest was *BRAF* for which mutations

Table 4. CNVs seen in UCD and HHV8$^-$/iMCD and FDSCs arising from UCD

Genes	Cases	CNV type	CNV exons	CNV ratio
UCD and MCD				
ETS1	3, 5	Gain	10 of 10	1.43
PTPN6	3, 5	Gain	16 of 17	1.39
TGFBR2	3, 5	Gain	8 of 8	1.45
TUSC3	3	Gain	9 of 11	1.4
IKZF3	5	Gain	8 of 9	1.47
PIM1	5	Gain	7 of 7	1.42
HIST genes	14	Gain	1 of 1	1.35-1.93
FDCSs				
BRAF	19, 20	Deletion	5 of 18; 8 of 18	−1.15
FANCB	19	Deletion	3 of 10	−1.17
FANCB	20	Gain	6 of 10	0.67
JAK2	19, 20	Deletion	4 of 25, 6 of 25	−1.15, −1.02
MAP3K5	19	Gain	3 of 30	1.22
MSH3	19	Deletion	2 of 24	−1.71
NFKB1	19	Deletion	4 of 24	−1.59
AR	20	Gain	8 of 8	1.2
HIST1H1D	20	Deletion	1 of 1	−0.69
HIST1H3A	20	Deletion	1 of 1	−0.68
HIST1H3E	20	Deletion	1 of 1	−0.68
MAP3K15	20	Gain	29 of 29	0.94
MED12	20	Gain	45 of 45	0.81
NPM1	20	Deletion	2 of 10	−0.75
VCAM1	21	Gain	5 of 9	0.86

in this gene have been described in a single research study of FDCSs by Go et al.[8] In our study, no *BRAF* mutations were seen. However, we identified copy-number aberrations (losses) in the *BRAF* gene in 2 of our FDCS cases.

We additionally evaluated for other genetic alterations such as copy-number changes and translocations in UCD, iMCD, and FDCS associated with UCD-HVV. Copy-number alterations were additionally seen in 3 cases of CD. Two cases, 1 of iMCD-PC (case 3) and an unusual UCD-MV (case 5) with multinodal involvement localized to the bilateral cervical chain, showed common amplification of *PTPN6*, *ETS1*, and *TGFBR2*. Although these genes do not share a common pathway, each is known to interface in oncogenesis or critical biologic processes relevant to UCD and iMCD in multiple systems. In mouse models, *PTPN6* plays a critical role in subsets of immune system cells and deletion of *PTPN6* results in alteration of dendritic cell function and features of autoimmunity; mice with null mutations in *PTPN6* present with splenomegaly, lymphadenopathy, and increased anti-nuclear antibodies. Both MCD and UCD can show abnormalities in follicular dendritic cells and clinical features that overlap with autoimmune disorders, though, in our case, amplification of *PTPN6* was seen rather than deletion.[7,34,35] Overexpression of *PTPN6* is seen in other diseases such as ovarian carcinoma and gliomas, leading to enhanced oncogenesis and more aggressive pathologic behavior.[36]

It is interesting to note that the 1 case of UCD (case 5) with amplification of *PTPN6* showed unusual multinodal involvement, localized to the bilateral cervical chain, with continued recurrence despite systemic treatment with anti–IL-6 therapies (tocilizumab); similarly, the patient with iMCD (case 3) and amplification of *PTPN6* failed to fully respond to targeted (anti-IL-6) and systemic (rituximab and etoposide) therapies. Amplification of *ETS1* was also present. *ETS1* is a known oncogene, and higher stromal and endothelial expression of this gene in carcinomas affects invasive properties.[37,38] That it is amplified in UCD (case 5) and iMCD (case 3) again is at least consistent with the more aggressive clinical course for these 2 patients. Finally, *ETS1* is further known to regulate angiogenesis; again, increased vascularization is a feature commonly seen in cases of iMCD and UCD.[39,40] Amplification of *TGFBR2* was also seen; a gene ubiquitously expressed, it is increased in relative quantity in stromal/vascular tissues and high expression is associated with poor prognosis in some cancer types.[41] Again, given the clinical course of the case of iMCD (case 3) and UCD (case 5), the amplification and tissue expression patterns are at least consistent with what might be expected based on our understanding of this gene.[42] One overarching hypothesis regarding how the amplification of *PTPN6*, *ETS1*, and *TGFBR2* might relate specifically to the pathogenesis of iMCD (case 3) and the more aggressive/relapsing case of UCD (case 5) may be that amplification of these genes in an unidentified neoplastic/clonal cell results in increased cellular proliferation (all of these genes affect cellular proliferation), which ultimately results in a paraneoplastic condition with increased cytokine production (ie, IL-6) from this clonal population and resultant polyclonal plasma cell proliferation from the expression of IL-6; we note that both cases showed a polyclonal plasma cell proliferation. Furthermore, the amplification of *TGFBR2* may specifically result in increases in IL-6 expression; activation of the TGFB2 pathway increases IL-6 expression in fibroblast cell lines in vitro and in in vivo mouse model systems.[43,44] Alternatively, individually, each gene amplification may play different roles in the pathogenesis of iMCD and UCD aside from what is noted here; again, further research is truly needed. However, we also note that CNV changes in specific genes, as other somatic mutations, may be passenger genetic abnormalities and not driver genetic abnormalities responsible for the disease; alternatively, these CNVs may be inherited and not de novo.

Amplification of the cluster of *HIST1H* genes on chromosome 6p was seen in an additional case of UCD-HVV (case 14). Amplification of HIST1H genes is a feature seen in uterine and ovarian carcinosarcomas, which have undergone gene expression toward a more mesenchymal state.[45] This case showed an increased stromal component as typical of UCD-HVV. As such, the amplification of *HIST1H* genes seen in the case of UCD-HVV may reflect transition of a clonal/neoplastic cell to a more mesenchymal phenotype necessarily resulting in either increased cellular proliferation or a readout of that proliferation.

Overall, genetic alterations in UCD and iMCD are not completely surprising given prior findings that at least a subset of UCD and iMCD cases show clonal origins by cytogenetic or other genetic assays.[6] However, most of our UCD-HVV cases did not show genetic alterations, which could be due to the sensitivity of our assays, or the targeted nature of our sequencing panel (405 of

20 000 genes), or could point to a different nonneoplastic etiology for a subset of cases, a supposition also proposed by Fajgenbaum et al and others.[3,7] It is interesting to note that the cases of UCD with CNV changes showed more aggressive behaviors and a relapsing/refractory clinical pattern. Lastly, TdT^+ T cells have been identified as increased in cases of UCD, MCD, and FDCS[46-48]; however, no association between genetic abnormalities and populations of TdT^+ T cells was seen in this study.

The cell of origin, resulting in UCD and iMCD disease, remains elusive. Currently based on limited studies, one hypothesis is that underlying stromal cells such as follicular dendritic cells are the clonal neoplastic cells, though this has not been fully confirmed.[6,7] In this study, we attempted to manually microdissect out individual cells, but attempts to manually isolate rare cells were nonproductive as amplification of DNA from old (>7 years old) tissues was an obstacle from very small populations of cells and our limited tissue was exhausted precluding further analysis of these cases. However, further prospective research using cutting-edge immunophenotypic and genetic technologies such as multiplexed ion beam imaging coupled with single-cell genetic analysis and laser-capture microdissection could be a source for determining and further evaluating the cell of origin.[49]

Finally, we also identified CNV changes in our FDCS cases. Among those, CNVs in genes previously described as altered in FDCS were noted, such as *NFKBI* and *JAK2*.[9] Cases 19 and 20 showed gene losses involving *JAK2*. We also saw copy-number deletions in the *HIST1H* genes in case 20, which also showed significant copy-number amplifications in *MAP3K15* and in *MED12*. Overall, a comparison of UCD and iMCD cases, with cases of FDCS associated with UCD-HVV, demonstrated rare genetic changes in 2 cases of UCD and 1 of iMCD (3 with CNVs and 1 iMCD with an additional *DNMT3A* somatic mutation), whereas all FDCS cases had significant somatic mutations (3-5 per case) and numerous CNVs. Our findings also suggest that additional genetic alterations are necessary for FDCS to arise in the setting of UCD. However, it is important to note that a targeted panel of 405 genes was evaluated for the UCD and iMCD cases whereas WES was performed for the FDCS cases.

There are several limitations of this study. First, it is largely observational, and we did not perform in vivo functional studies to address how specifically these genetic alterations result in the phenotypic manifestations of UCD, iMCD, and FDCS. Additionally, with respect to UCD and iMCD, though we postulate that these genetic abnormalities reside in a clonal/neoplastic population of cells, we and others have not identified this specific cell, though evidence from other studies points to a stromal population of cells. Finally, although we did perform a broad DNA mutational analysis of 405 genes in UCD and iMCD cases, we did not interrogate all genes, intronic regions, nor translocations fully.

To the best of our knowledge, our study is the first to analyze the genetic and epigenetic features of UCD and iMCD, and FDCS associated with UCD-HVV. Our findings are compelling and clearly point to a future direction of needed work to decipher the molecular pathogenesis of these diseases.

Acknowledgment

This work was supported by research awards (R.S.O.) from Foundation Medicine and Agilent Technologies.

Authorship

Contribution: R.S.O. conceived of and designed the study, analyzed data, and wrote the manuscript; S.A. conceived of and designed the study, analyzed data, and edited the manuscript; A.N. performed research, designed experiments, analyzed data, and wrote the manuscript; A.B., N.S., J.S., J.L.Z., T.M., and R.A.W. analyzed data and edited the manuscript; and all authors reviewed the drafts and the final version of the manuscript.

Conflict-of-interest disclosure: T.M. and S.A. are employees of Foundation Medicine and have equity interest. The remaining authors declare no competing financial interests.

ORCID profile: R.S.O., 0000-0003-1881-3440.

Correspondence: Robert S. Ohgami, Department of Pathology, Stanford University, 300 Pasteur Dr, Room L235, Stanford, CA 94305; e-mail: rohgami@stanford.edu.

References

1. Waterston A, Bower M. Fifty years of multicentric Castleman's disease. *Acta Oncol*. 2004;43(8):698-704.
2. Casper C. The aetiology and management of Castleman disease at 50 years: translating pathophysiology to patient care. *Br J Haematol*. 2005;129(1):3-17.
3. Takai K, Nikkuni K, Shibuya H, Hashidate H. Thrombocytopenia with fever, chest ascites, hepatosplenomegaly, mild fibrosis in the bone marrow. *Rinsho Ketsueki*. 2010;51:320-325.
4. Kawabata H, Takai K, Kojima M, et al. Castleman-Kojima disease (TAFRO syndrome): a novel systemic inflammatory disease characterized by a constellation of symptoms, namely, thrombocytopenia, ascites (anasarca), microcytic anemia, myelofibrosis, renal dysfunction, and organomegaly: a status report and summary of Fukushima (6 June, 2012) and Nagoya meetings (22 September, 2012). *J Clin Exp Hematop*. 2013;53(1):57-61.
5. Iwaki N, Fajgenbaum DC, Nabel CS, et al. Clinicopathologic analysis of TAFRO syndrome demonstrates a distinct subtype of HHV-8-negative multicentric Castleman disease. *Am J Hematol*. 2016;91(2):220-226.
6. Chang KC, Wang YC, Hung LY, et al. Monoclonality and cytogenetic abnormalities in hyaline vascular Castleman disease. *Mod Pathol*. 2014;27(6):823-831.
7. Fajgenbaum DC, van Rhee F, Nabel CS. HHV-8-negative, idiopathic multicentric Castleman disease: novel insights into biology, pathogenesis, and therapy. *Blood*. 2014;123(19):2924-2933.
8. Go H, Jeon YK, Huh J, et al. Frequent detection of BRAF(V600E) mutations in histiocytic and dendritic cell neoplasms. *Histopathology*. 2014;65(2):261-272.

9. Griffin GK, Sholl LM, Lindeman NI, Fletcher CDM, Hornick JL. Targeted genomic sequencing of follicular dendritic cell sarcoma reveals recurrent alterations in NF-κB regulatory genes. *Mod Pathol*. 2016;29(1):67-74.

10. Ozawa MG, Bhaduri A, Chisholm KM, et al. A study of the mutational landscape of pediatric-type follicular lymphoma and pediatric nodal marginal zone lymphoma. *Mod Pathol*. 2016;29(10):1212-1220.

11. Ungewickell A, Bhaduri A, Rios E, et al. Genomic analysis of mycosis fungoides and Sézary syndrome identifies recurrent alterations in TNFR2. *Nat Genet*. 2015;47(9):1056-1060.

12. He J, Abdel-Wahab O, Nahas MK, et al. Integrated genomic DNA/RNA profiling of hematologic malignancies in the clinical setting. *Blood*. 2016;127(24):3004-3014.

13. Fajgenbaum DC, Uldrick TS, Bagg A, et al. International, evidence-based consensus diagnostic criteria for HHV-8-negative/idiopathic multicentric Castleman disease. *Blood*. 2017;129(12):1646-1657.

14. Maeda T, Merghoub T, Hobbs RM, et al. Regulation of B versus T lymphoid lineage fate decision by the proto-oncogene LRF. *Science*. 2007;316(5826):860-866.

15. Andersson E, Kuusanmäki H, Bortoluzzi S, et al. Activating somatic mutations outside the SH2-domain of STAT3 in LGL leukemia. *Leukemia*. 2016;30(5):1204-1208.

16. Jerez A, Clemente MJ, Makishima H, et al. STAT3 mutations unify the pathogenesis of chronic lymphoproliferative disorders of NK cells and T-cell large granular lymphocyte leukemia. *Blood*. 2012;120(15):3048-3057.

17. Koskela HL, Eldfors S, Ellonen P, et al. Somatic STAT3 mutations in large granular lymphocytic leukemia. *N Engl J Med*. 2012;366(20):1905-1913.

18. Zhang W, Xu J. DNA methyltransferases and their roles in tumorigenesis. *Biomark Res*. 2017;5(1):1.

19. Yang L, Rau R, Goodell MA. DNMT3A in haematological malignancies. *Nat Rev Cancer*. 2015;15(3):152-165.

20. Quek L, Ferguson P, Metzner M, et al. Mutational analysis of disease relapse in patients allografted for acute myeloid leukemia. *Blood Adv*. 2016;1(3):193-204.

21. Dhayalan A, Rajavelu A, Rathert P, et al. The Dnmt3a PWWP domain reads histone 3 lysine 36 trimethylation and guides DNA methylation. *J Biol Chem*. 2010;285(34):26114-26120.

22. Chen T, Tsujimoto N, Li E. The PWWP domain of Dnmt3a and Dnmt3b is required for directing DNA methylation to the major satellite repeats at pericentric heterochromatin. *Mol Cell Biol*. 2004;24(20):9048-9058.

23. Challen GA, Sun D, Jeong M, et al. Dnmt3a is essential for hematopoietic stem cell differentiation. *Nat Genet*. 2011;44(1):23-31.

24. Wu H, Zeng H, Lam R, et al. Structural and histone binding ability characterizations of human PWWP domains. *PLoS One*. 2011;6(6):e18919.

25. Yang F, Zhou S, Wang C, et al. Epigenetic modifications of interleukin-6 in synovial fibroblasts from osteoarthritis patients. *Sci Rep*. 2017;7:43592.

26. Suematsu S, Matsuda T, Aozasa K, et al. IgG1 plasmacytosis in interleukin 6 transgenic mice. *Proc Natl Acad Sci USA*. 1989;86(19):7547-7551.

27. Jaiswal S, Fontanillas P, Flannick J, et al. Age-related clonal hematopoiesis associated with adverse outcomes. *N Engl J Med*. 2014;371(26):2488-2498.

28. Genovese G, Kähler AK, Handsaker RE, et al. Clonal hematopoiesis and blood-cancer risk inferred from blood DNA sequence. *N Engl J Med*. 2014;371(26):2477-2487.

29. Hartmann L, Dutta S, Opatz S, et al. ZBTB7A mutations in acute myeloid leukaemia with t(8;21) translocation. *Nat Commun*. 2016;7:11733.

30. Yu H, Lee H, Herrmann A, Buettner R, Jove R. Revisiting STAT3 signalling in cancer: new and unexpected biological functions. *Nat Rev Cancer*. 2014;14(11):736-746.

31. Ohgami RS, Ma L, Monabati A, Zehnder JL, Arber DA. STAT3 mutations are present in aggressive B-cell lymphomas including a subset of diffuse large B-cell lymphomas with CD30 expression. *Haematologica*. 2014;99(7):e105-e107.

32. Ohgami RS, Ma L, Merker JD, Martinez B, Zehnder JL, Arber DA. STAT3 mutations are frequent in CD30+ T-cell lymphomas and T-cell large granular lymphocytic leukemia. *Leukemia*. 2013;27(11):2244-2247.

33. Wu A, Pullarkat S. Follicular dendritic cell sarcoma. *Arch Pathol Lab Med*. 2016;140(2):186-190.

34. Abram CL, Roberge GL, Pao LI, Neel BG, Lowell CA. Distinct roles for neutrophils and dendritic cells in inflammation and autoimmunity in motheaten mice. *Immunity*. 2013;38(3):489-501.

35. Luo JM, Li S, Huang H, et al. Clinical spectrum of intrathoracic Castleman disease: a retrospective analysis of 48 cases in a single Chinese hospital. *BMC Pulm Med*. 2015;15(1):34.

36. Mok SC, Kwok TT, Berkowitz RS, Barrett AJ, Tsui FW. Overexpression of the protein tyrosine phosphatase, nonreceptor type 6 (PTPN6), in human epithelial ovarian cancer. *Gynecol Oncol*. 1995;57(3):299-303.

37. Behrens P, Mathiak M, Mangold E, et al. Stromal expression of invasion-promoting, matrix-degrading proteases MMP-1 and -9 and the Ets 1 transcription factor in HNPCC carcinomas and sporadic colorectal cancers. *Int J Cancer*. 2003;107(2):183-188.

38. Trojanowska M. Ets factors and regulation of the extracellular matrix. *Oncogene*. 2000;19(55):6464-6471.

39. Garrett-Sinha LA. Review of Ets1 structure, function, and roles in immunity. *Cell Mol Life Sci*. 2013;70(18):3375-3390.

40. Testoni M, Chung EY, Priebe V, Bertoni F. The transcription factor ETS1 in lymphomas: friend or foe? *Leuk Lymphoma*. 2015;56(7):1975-1980.

41. Barlow J, Yandell D, Weaver D, Casey T, Plaut K. Higher stromal expression of transforming growth factor-beta type II receptors is associated with poorer prognosis breast tumors. *Breast Cancer Res Treat*. 2003;79(2):149-159.

42. Owens GK, Kumar MS, Wamhoff BR. Molecular regulation of vascular smooth muscle cell differentiation in development and disease. *Physiol Rev*. 2004; 84(3):767-801.

43. Novitskiy SV, Forrester E, Pickup MW, et al. Attenuated transforming growth factor beta signaling promotes metastasis in a model of HER2 mammary carcinogenesis. *Breast Cancer Res*. 2014;16(5):425.

44. Elias JA, Lentz V, Cummings PJ. Transforming growth factor-beta regulation of IL-6 production by unstimulated and IL-1-stimulated human fibroblasts. *J Immunol*. 1991;146(10):3437-3443.

45. Zhao S, Bellone S, Lopez S, et al. Mutational landscape of uterine and ovarian carcinosarcomas implicates histone genes in epithelial-mesenchymal transition. *Proc Natl Acad Sci USA*. 2016;113(43):12238-12243.

46. Ohgami RS, Sendamarai AK, Atwater SK, et al. Indolent T-lymphoblastic proliferation with disseminated multinodal involvement and partial CD33 expression. *Am J Surg Pathol*. 2014;38(9):1298-1304.

47. Ohgami RS, Arber DA, Zehnder JL, Natkunam Y, Warnke RA. Indolent T-lymphoblastic proliferation (iT-LBP): a review of clinical and pathologic features and distinction from malignant T-lymphoblastic lymphoma. *Adv Anat Pathol*. 2013;20(3):137-140.

48. Ohgami RS, Zhao S, Ohgami JK, et al. TdT+ T-lymphoblastic populations are increased in Castleman disease, in Castleman disease in association with follicular dendritic cell tumors, and in angioimmunoblastic T-cell lymphoma. *Am J Surg Pathol*. 2012;36(11):1619-1628.

49. Rost S, Giltnane J, Bordeaux JM, Hitzman C, Koeppen H, Liu SD. Multiplexed ion beam imaging analysis for quantitation of protein expression in cancer tissue sections. *Lab Invest*. 2017;0:1-12.